Characterization of Soluble and Membrane-Bound Family 3 Lytic Transglycosylases from *Pseudomonas aeruginosa*†

Neil T. Blackburn and Anthony J. Clarke*

Department of Microbiology, University of Guelph, Guelph, Ontario N1G 2W1, Canada

Received September 24, 2001; Revised Manuscript Received November 2, 2001

ABSTRACT: Lytic transglycosylases cleave the β,1→4 glycosidic linkages between the *N*-acetylmuramoyl (MurNAc) and *N*-acetylglucosaminyl (GlcNAc) residues of peptidoglycan with the concomitant formation of 1,6-anhydro-*N*-acetylmuramyl reaction products. The genes encoding two hypothetical lytic transglycosylases were identified in the genome of *Pseudomonas aeruginosa* PAO1 by a BLAST search using membrane-bound lytic transglycosylase B (MltB) from *Escherichia coli* as the query. The two genes were amplified by PCR and cloned as fusion proteins with C-terminal hexa-His sequences. Expression studies of the two genes in *E. coli* in the presence of [^{3}H]palmitate resulted in the labeling of only one of the two enzymes. This enzyme, named MltB, was overexpressed to form insoluble inclusion bodies. Its gene was engineered to produce a truncated form of the enzyme lacking its N-terminal 17 residues which includes Cys17, the putative site of lipidation. This MltB derivative (named sMltB) was shown to not label with [^{3}H]palmitate, and it was overexpressed in soluble form. The second, nonlabeled enzyme was overexpressed in soluble form and hence was named soluble lytic transglycosylase B (SltB). Both sMltB and SltB were purified to apparent homogeneity by a combination of affinity (Ni^{2+}-NTA), cation-exchange (Mono S), and gel permeation (Superdex 75) chromatographies. The reaction products released by the two enzymes from purified, insoluble peptidoglycan were characterized by a novel high-performance anion-exchange chromatography (HPAEC) assay. Both enzymes produced the same three major soluble products which were identified as anhydromuropeptides based on ESI-MS analysis (cross-linked anhydrodisaccharide-tetrasaccharide, *m*/*z* obs 1824.9; anhydrodisaccharide-pentapeptide, *m*/*z* obs 922.2; and anhydrodisaccharide-tripeptide, *m*/*z* obs 851.3. The Michaelis−Menten kinetic parameters were also determined for the two enzymes using the same insoluble peptidoglycan substrate by aminosugar compositional analysis of soluble reaction products. At pH 5.8 and in the presence of 0.1% Triton, SltB was found to be more catalytically efficient, as reflected by its k_{cat}/K_M value, than sMltB.

Bacteria withstand the strong, outward-facing turgor pressure on their cytoplasmic membranes by possessing an exoskeleton known as the murein or peptidoglycan sacculus. This covalently closed macromolecule completely surrounds the cytoplasmic membrane and is composed of glycan strands of two alternating amino sugars, *N*-acetylmuramic acid (MurNAc)[1] and *N*-acetylglucosamine (GlcNAc). The glycan strands are interconnected by short stem peptides generating the three-dimensional sacculus of carbohydrate and amino acids (reviewed in *1*). The well-characterized biosynthetic pathway of peptidoglycan culminates in the incorporation of muropeptide repeating units into the existing sacculus through the activities of the periplasmic penicillin-binding proteins (PBPs) (reviewed in *2*). However, to accommodate cell elongation and division activities, the sacculus must have the capacity to be reshaped during growth. Peptidoglycan-cleaving enzymes or autolysins are thought to allow this reshaping to occur, and enzymes have been found that cleave most of the bonds within peptidoglycan (*3*−*5*).

The lytic transglycosylases (LTs) represent one class of autolysins, and they act like hen egg-white lysozyme (EC 3.2.1.17; peptidoglycan *N*-acetylmuramoylhydrolase), a muramidase that cleaves the β,1→4 glycosidic linkages between MurNAc and GlcNAc residues (*6*). However, unlike muramidases which are hydrolytic enzymes, LTs are peptidoglycan transferases (EC 2.4.1.*X*) catalyzing the cleavage of the glycosidic bonds with the concomitant formation of 1,6-anhydromuramoyl residues (AnhMurNAc) (Figure 1). This feature is of great significance because released fragments of peptidoglycan containing 1,6-anhydromuramic acid have been shown to cause a variety of pathobiological effects. For example, GlcNAc-AnhMurNAc-tetrapeptide is released by *Bordatella pertussis*, the etiological agent of whooping cough, and this muropeptide (also known as tracheal autotoxin) has been shown to induce cell damage in the

† This work was supported by operating grants to A.J.C. from the Natural Sciences and Engineering Council of Canada and the Canadian Bacterial Diseases Network, a National Centre of Excellence, and by a studentship to N.T.B. from the Natural Sciences and Engineering Research Council of Canada.

* Address correspondence to this author at the Department of Microbiology, University of Guelph, Guelph, Ontario N1G 2W1, Canada. Phone: 1-519-824-4120 (ext. 3361), Fax: 1-519-837-1802, E-mail: aclarke@micro.uoguelph.ca.

[1] Abbreviations: MurNAc, *N*-acetylmuramic acid; GlcNAc, *N*-acetylglucosamine; PBP, penicillin-binding protein; LT, lytic transglycosylase; AnhMurNAc, 1,6-anhydro-*N*-acetylmuramic acid; Mlt, membrane-bound lytic transglycosylase; sMlt, soluble derivative of membrane-bound lytic transglycosylase; Slt, soluble lytic transglycosylase; HPAEC, high-pH anion-exchange chromatography;

10.1021/bi011833k CCC: $22.00
Published on Web 12/21/2001

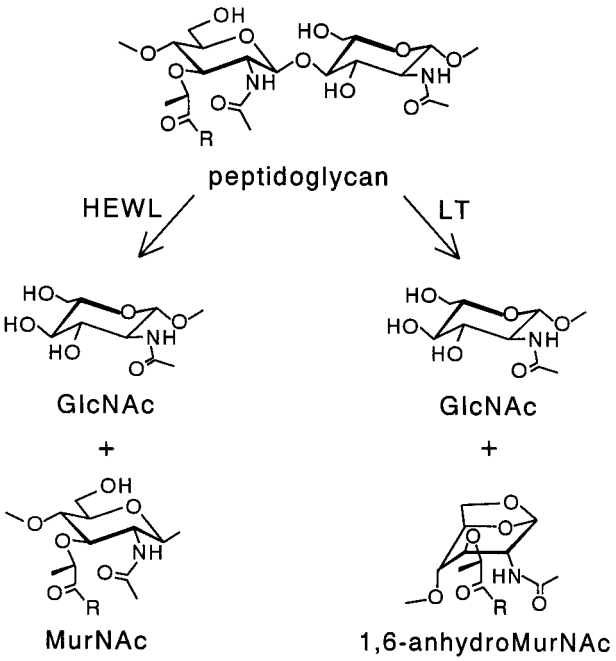

FIGURE 1: Comparison of lysozyme (HEWL) and lytic transglycosylase (LT) cleavage reactions. R represents the stem peptide attached to the lactyl group at C-3 of MurNAc.

respiratory tract as observed during infection by *B. pertussis* (*7*). A variety of other apparent effects of 1,6-anhydromuropeptides include pyrogenicity, somnogenicity, and the induction of rheumatoid arthritis and complement activation (reviewed in *6*, *8*).

In addition to the diverse effects of their reaction products, the presumed mechanism of action of the LTs is very interesting. Like most other glycosidases which function using either a single- or double-displacement reaction mechanism, hen egg-white lysozyme possesses a catalytic diad of acidic residues (*9*). Glu35 remains protonated at physiological pH to act as a catalytic acid/base, while deprotonated Asp52 serves as a nucleophile to stabilize the putative oxocarbenium transition state formed during hydrolysis (*10*). In contrast, LTs appear to catalyze cleavage involving only a single acidic residue. Thus, in the LTs studied to date, a glutamyl residue is thought to first donate a proton to the glycosidic oxygen of the linkage to be cleaved, followed by abstraction of the C-6 hydroxyl group proton of the oxocarbenium ion intermediate leading to the formation of 1,6-andydromuramic acid (Figure 2). The glycosyl hydrolase family 20 β-*N*-acetylhexosaminidases (EC 3.2.1.52, β-*N*-acetyl-D-hexosaminide *N*-acetylhexosaminohydrolase), the functionally related family 18 chitinases [EC 3.2.1.14, poly-(1,4-(*N*-acetyl-β-D-glucosaminide)) glycanohydrolase], and the family 23 goose-type lysozymes also appear to function with a single catalytic residue (*11*−*13*), but these hydrolases do not form anhydrosugar products (*8*). Several lines of evidence suggest that these latter enzymes invoke substrate-assisted catalysis using the *N*-acetyl group of substrate which forms an oxazoline transition state to substitute for a stabilizing anion on the enzyme (*11*, *12*, *14*). We propose that the LTs would function in a similar manner but instead of hydrolysis, the oxazoline intermediate would be attacked intramolecularly by its C-6 oxygen. Thus, the distinct activity of LTs among peptidoglycan-degrading enzymes makes them an attractive antimicrobial target as a mechanism-based

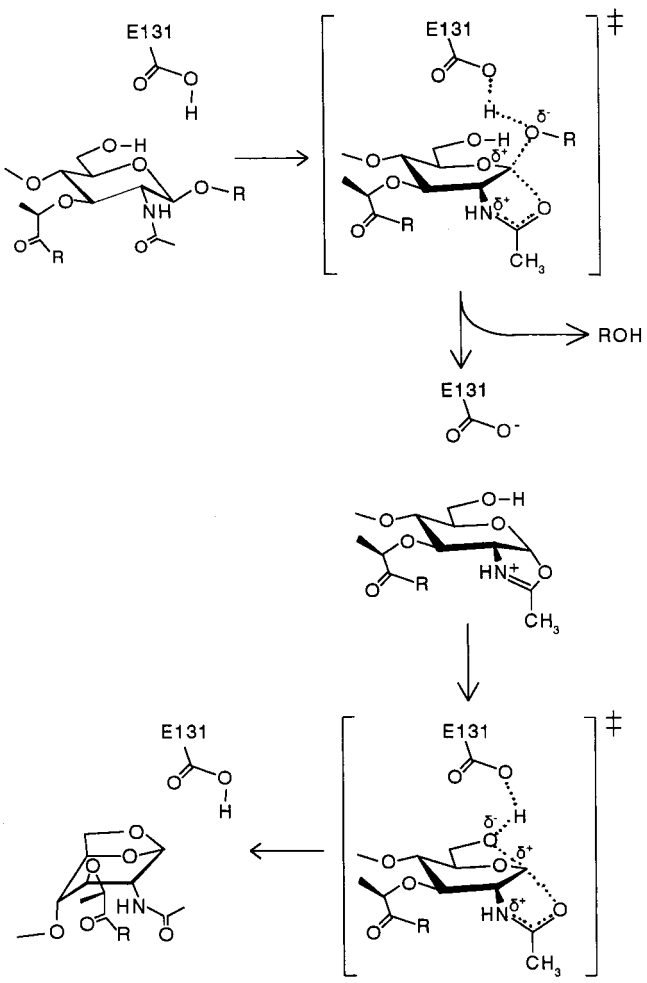

FIGURE 2: Proposed reaction mechanism of SltB1 and MltB. Glu131 (SltB1) or Glu162 (MltB) serve initially as an acid to protonate the glycosidic linkage to be cleaved leading to the formation of the muramoyloxazoline intermediate, and then as a base to abstract the C-6 hydroxyl proton promoting collapse of the oxazoline and concomitant formation of the 1,6-anhydromuramoyl product.

inhibitor should not interfere with innate immunity, i.e., human lysozyme.

LTs appear to be ubiquitous in eubacteria that produce peptidoglycan (viz., all but the cell wall-less mycoplasmas), and even in some lytic bacteriophages (*15*). Alignment of known and hypothetical LT proteins from microbial genome databases at the National Center for Biotechnology Information has allowed their arrangement into four families based on differences within consensus signature sequences around their core catalytic domains (*15*). LT family 3 has as its prototypical enzyme the membrane-bound lytic transglycosylase B (MltB) from *Escherichia coli* (*16*, *17*). MltB of *E. coli* is a 38 kDa outer membrane-localized protein which contains a lipoprotein-processing site that can be labeled with [^{3}H]palmitate. Overexpression of this protein in *E. coli* led to rapid cell lysis and a 55-fold increase in murein hydrolase activity, indicating that the induced protein was exported to the periplasm (*17*). *E. coli* also contains a naturally produced soluble cleavage product of MltB called Slt35 (for soluble lytic transglycosylase) (*16*, *18*).

The crystal structure of Slt35 at 1.7 Å resolution has revealed that this protein contains a lysozyme-like fold in its catalytic domain (*19*). The only other bacterial LT for

Table 1: Bacterial Strains and Plasmids Used in This Study

strain or plasmid	genotype or relevant characteristic	ref or source
E. coli strains		
DH5α	K-12 φ80d *lacZ*_M15 *endA1 hsdR17* (r_K^- m_K^-) *supE44 thi-1 gyrA96 relA1* ρ(*lacZYA-argF*) U169 F^-	Clontech
BL21[λDE3] pLysS	F^-*ompT hsdS*$_B$ (r_B^- m_B^-) *gla dcm met* (DE3) pLysS (Cm^R)	Novagen
SM10	*thi*−1 *thr leu ton*A *lacy sup*E *rec*A RP4−2-Tc::Mu, Km^R	*23*
P. aeruginosa strains		
PAO1	serotype O5	*50*
PAO1-ρ*mltB*	PAO1 derivative; ρ*mltB*::Gm^R	this study
PAO1-ρ*sltB*1	PAO1 derivative; ρ*sltB1*::Gm^R	this study
plasmids		
pET30a(+)	IPTG inducible expression vector; Km^R	Novagen
PUCGM	source of Gm^R cassette for chromosomal mutation	*21*
pEX18Ap	gene replacement vector, Ap^R *ori*T^+ *sac*B^+	*22*
pNBAC 299-12	pET30a(+) derivative containing *mlt*B on a *Nde*I/*Xho*I fragment; Kan^R	this study
pNBAC 54-1	pET30a(+) derivative containing *mlt*B on a *Nde*I/*Xho*I fragment encoding an N-terminal trucation of Arg-2 to Cys-17; Kan^R	this study
pNBAC 258-2	pET30a(+) derivative containing *slt*B1 on a *Nde*I/*HindIII* fragment; Kan^R	this study
pNTB-100	pNBAC 299-12 derivative containing Gm^R cassette from pUCGM; Gm^R	this study
pNTB-101	pEX18Ap derivative containing *mltB*::Gm^R; Kan^R, Gm^R	this study
pNTB-200	pNBAC 258−2 derivative containing Gm^R cassette from pUCGM; Gm^R	this study
pNTB-201	pEX18Ap derivative containing *sltB1*::Gm^R; Kan^R, Gm^R	this study

which structural data exist is Slt70 of *E. coli* (*20*, *21*). Slt70 also contains a lysozyme-fold catalytic domain despite not sharing any sequence similarity with Slt35. Cocrystallization of Slt35 with *N*-(acetylglucosamyl)-*N*-(acetylmuramoyl)-L-alanine-D-glutamic acid led to the identification of four sugar-binding subsites within the enzyme and a putative catalytic Glu162 poised between the −1 and +1 binding sites (*22*). This crystal structure revealed that Slt35 has an 'exo-loop' near the substrate-binding cleft that is believed to block any endo-glycosidase cleavage of peptidoglycan and impose a strict exo-activity by this LT. Slt35 also contains a helix−loop−helix domain with strong similarity to the eukaryotic EF-hand calcium-binding fold. Circular dichroism measurements have shown that binding of Ca^{2+} to Slt35, presumably through the EF-hand, assist in the temperature stability of the enzyme in vitro (*23*).

Amino acid sequence alignment studies using the single MltB from *E. coli* as a probe suggests that *Pseudomonas aeruginosa*, a Gram-negative, human opportunistic pathogen often associated with morbidity and mortality among cystic fibrosis patients (*24*), has four family 3 LTs (*15*). The most homologous *P. aeruginosa* family 3 homologue shares 66% amino acid identity with the *E. coli* enzyme, and includes a lipoprotein processing site. As we show herein that this homologue is a lipoprotein, we have also named it MltB (pseudomonas genome project annotation no. PA4444). The other three homologues are 41%, 34%, and 31% identical to the *E. coli* enzyme, but they do not contain a predicted lipidation site. Thus, these hypothetical enzymes are named SltB1 (annotation no. PA4001), SltB2 (annotation no. PA1171), and SltB3 (annotation no. PA3992), respectively. All four family 3 enzymes from *P. aeruginosa* contain an invariant glutamyl residue homologous to Glu162, and all contain a hypothetical EF-hand motif (*15*).

In this study, we describe the cloning and overexpression of the genes encoding MltB and SltB1 from *P. aeruginosa*. These gene products were purified to apparent homogeneity to provide the first report of Michaelis−Menten kinetic parameters for any LT and thereby characterize differences in their enzymatic properties.

EXPERIMENTAL PROCEDURES

Reagents, Bacterial Strains, and Growth Conditions. Unless stated otherwise, all chemicals, growth media, and reagents were from Sigma Chemical Co. (St. Louis, MO), while restriction enzymes were from New England Biolabs (Mississauga, ON). The sources of plasmids and bacterial strains used in this study, together with their description, are listed in Table 1. *P. aeruginosa* PAO1, *E. coli* DH5α, and SM10 were maintained on LB broth or agar which was supplemented with 30 μg/mL kanamycin sulfate in the case of pET30a(+) (Novagen)-containing strains. *Pseudomonas* isolation agar (Difco) was also used to grow PAO1 during construction of chromosomal mutants of lytic transglycosylases. *E. coli* BL21-λDE3 (pLysS) (Novagen) used for protein expression was maintained on LB agar containing 34 μg/mL chloramphenicol. All bacteria were grown at 37 °C, unless otherwise stated.

Ostrich (*Struthio camelus*) egg-white lysozyme was purified from a single egg to apparent homogeneity, as determined by SDS−PAGE, by a combination of cation-exchange chromatography and gel filtration as previously described by Jollès et al. (*25*). Mutanolysin and hen egg-white lysozyme were obtained from Sigma.

Cloning of Lytic Transglycosylase Genes from P. aeruginosa. The *Pseudomonas* genome project (http://www.pseudomonas.com) was used to identify homologous open reading frames (ORFs) within strain PAO1 to lytic transglycosylases from *E. coli* and to design oligonucleotide primers for PCR amplification. Chromosomal DNA template for PCR was isolated from strain PAO1 in the presence of hexadecyltrimethylammonium bromide (*26*). Full-length *mltB* was amplified using primers 5′-AAGACCCCATATGCGC-

CGTACCGCCCT-3′ and 5′-TCTCGAGGTGCGAATCCT-GCCTGACG-3′ which contain *Nde*I and *Xho*I, sites respectively (underlined), to facilitate cloning. Truncated *mltB* was amplified from the same template DNA and downstream primer as the full-length product; however, the upstream primer was modified to 5′-GTCTCACATATGAGCAGC-CAACCGAC-3′ which contains an *Nde*I site. Full-length *sltB1* was amplified from PAO1 chromosomal DNA using the following primers: 5′-GAAGAACATATGCAAGTACT-GCGTACATG-3′ and 5′-GGAAAAGCTTGCGTGAATGGG-CACCTCG-3′, which contain *Nde*I and *Hin*dIII, sites, respectively. Amplified open reading frames were digested with restriction enzymes and ligated to appropriately digested pET30a(+) plasmid DNA and transformed into *E. coli* DH5α. After screening transformants for the correct size insert, the resulting isolated constructs were named pNBAC299-12 (full-length *mltB*), pNBAC54-5 (truncated *mltB*), and pNBAC258-1 (full-length *sltB1*). The nucleotide sequences of all three constructs including the plasmid-encoded hexa-histidine tag at the C-terminus of all three translated proteins were confirmed prior to protein expression experiments.

Chromosomal Mutation of Lytic Transglycosylase Genes. The allelic exchange strategy described by Schwiezer and Hoang (*26*) was used to construct chromosomal mutants in the *mltB* and *sltB1* ORFs in strain PAO1. For construction of the *mltB* mutant, plasmid pNBAC299-12 was digested at a unique *Eco*RI site within the *mltB* ORF. After generation of compatible ends with Klenow enzyme, the digested plasmid was ligated to an 855 bp *Sma*I fragment of plasmid pUCGM (*27*), which contained a gentamicin-resistance cassette, resulting in plasmid construct pNTB-100. Next, a 2004 bp *Xba*I−*Xho*I fragment of pNTB-100 containing the gentamicin-resistance cassette-interrupted *mltB* ORF was ligated to *Xba*I−*Sal*I digested pEX18Ap suicide vector (*28*) and designated pNTB-101. The pNTB-101 construct was introduced into the mobilizer strain *E. coli* SM10 by electroporation and then conjugally transferred into PAO1 using the method described by Simon et al. (*23*). Selection of recombinant PAO1, which had undergone gene replacement, was achieved by screening on PIA media for resistance to 300 μg/mL gentamicin (cassette marker) and sensitivity to 5% sucrose (due to the loss of *sacB* from pEX18Ap). Both true recombinants and merodiploids (gentamicin and sucrose resistant) were observed, but only the former were chosen for further study. The presence and orientation of the gentamicin cassette within the *mltB* ORF was confirmed by PCR and nucleotide sequencing using chromosomal DNA prepared from the mutant strain and the original cloning primers. A similar strategy was used to construct a *sltB1* mutant except pNBAC258-1 was digested at a unique *Msc*I site within the *sltB1* ORF and ligated to the 855 bp *Sma*I fragment of pUCGM to create pNTB-200. A 1926 bp fragment containing the gentamicin-resistance cassette-interrupted *sltB1* ORF was digested from pNTB-200 with *Xba*I−*Xho*I and ligated to *Xba*I−*Sal*I digested pEX18Ap to create pNTB-201. Transfer of this construct to PAO1 and selection of mutant *sltB1* were as described above.

Purification of Lytic Transglycosylases. *E. coli* BL21-λDE3 (pLysS) freshly transformed with plasmid DNA was inoculated into super broth (*24*) supplemented with 30 μg/mL kanamycin and 34 μg/mL chloramphenicol and incubated at 37 °C until early exponential phase. Cells were cooled to 18 °C for 15 min prior to the addition of IPTG (freshly prepared in water and filter sterilized) to a final concentration of 0.1 mM. Induced cells were incubated for up to 3 h at 18 °C and collected by centrifugation (5000*g*, 15 min, 4 °C). Cells were washed and resuspended in IMAC buffer [50 mM NaH_2PO_4, pH 8.0, 300 mM NaCl, 10% (w/v) glycerol, and 0.1% Triton X-100] containing CompleteJ EDTA-free protease inhibitor cocktail tablets (Roche Diagnostics, Laval PQ). Cells were disrupted using a Sonicator Ultrasonic Liquid Processor (Heat Systems Inc., Toronto, ON) fitted with a macroprobe set to 50% maximal output. Soluble cell fractions collected after centrifugation of cell lysates (5000*g*, 20 min, 4 °C) were mixed with Ni−NTA agarose (Qiagen, Valencia, CA) and incubated with shaking for 1 h at 4 °C. The resulting slurries were packed into a 1 cm × 10 cm disposable columns, and the flow through fractions were collected. Columns were washed with 10 column volumes of IMAC buffer, and the bound enzymes were eluted in 1 column volume of IMAC buffer with decreasing pH ranging from 7.5 to 5.5. For further purification, IMAC fractions containing enzyme were subjected to cation-exchange chromatography on Mono S 5/5 (Amersham Pharmacia Biotech, Uppsala, Sweden). Enzyme preparations were applied to Mono S in 10 mM ammonium acetate, pH 8.0, containing 0.1% Triton at 0.7 mL/min and recovered by application of a linear gradient to 1 M ammonium acetate containing 0.1% Triton over 30 min. Enzyme-containing fractions were desalted by gel filtration on Superdex-75 (Amersham Pharmacia Biotech) in 10 mM ammonium acetate, pH 8.0, containing 0.1% Triton at a flow rate of 1.0 mL/min.

[^{3}H]Palmitate Labeling of Lytic Transglycosylases. The labeling of lipoprotein was essentially as described elsewhere with slight modifications (*31*). Overnight cultures of plasmid-containing *E. coli* BL21-λDE3 (pLysS) cells grown in LB with 30 μg/mL kanamycin and 34 μg/mL chloramphenicol were used to inoculate fresh medium and then incubated at 37 °C until the OD_{600} reached 0.6. Some samples were then induced to express enzyme by the addition of 0.1 mM IPTG. The expression of lipoprotein was monitored by the addition of 5 μCi/mL [^{3}H]palmitate (60 Ci/mmol; American Radiolabeled Chemicals, St. Louis, MO). In addition, globomycin was added to some cultures at a final concentration of 100 μg/mL 5 min prior to the addition of radiolabel and/or IPTG. Cells were incubated for 1 h at 37 °C after which they were collected by centrifugation (5000*g*, 15 min, 4 °C). Cell pellets were washed twice in ice-cold 25 mM sodium phosphate buffer, pH 6.8, with 125 mM NaCl and lysed in 20 mM Tris-HCl, pH 8.0, containing 1 mM EDTA and 1% SDS by boiling for 10 min. After centrifugation to remove unlysed cells and insoluble material, protein in the supernatant was precipitated by the addition of ice-cold acetone and incubated overnight at −20 °C. The precipitated material was resuspended in 1% SDS, and aliquots of 10^6 cpm were separated on 12% or 15% SDS−PAGE gels. After electrophoresis, gels were immersed in Amplify (Amersham Pharmacia Biotech) and dried. Labeled lipoproteins were detected by fluorography using Hyperfilm MP (Amersham Pharmacia Biotech).

Western Immunoblotting. Detection of expressed enzymes took advantage of the C-terminal His-tag present on the enzyme by using a commercially available anti-tag antibody. All incubation steps for Western blot analysis were per-

formed at room temperature. Cell lysate samples radiolabeled with [^{3}H]palmitate were resolved by SDS−PAGE and transferred to nitrocellulose membranes using a BioRad mini-electroblotting apparatus (BioRad Laboratories, Inc., Mississauga, ON). The proteins were transferred in 10 mM $NaHCO_3$, 3 mM Na_2CO_3, and 20% methanol for 1 h at 50 V. The membrane was then washed twice in TBS buffer (10 mM Tris-HCl, pH 7.5, 150 mM NaCl) for 10 min. The membrane was blocked in TBS containing 3% BSA for 1 h and washed for 20 min in wash buffer (20 mM Tris-HCl, pH 7.5, 500 mM NaCl, 0.05% Tween-20, and 0.2% Triton X-100). The blot was then incubated in blocking solution containing a 1:100 dilution of mouse anti-hexa-His antibody (Qiagen, Valencia, CA) for 1 h. Next, the blot was washed twice in wash buffer and once in TBS for 10 min each. Goat anti-mouse IgG + IgM alkaline phosphatase conjugated antibody (Caltag Laboratories, Burlingame, CA) diluted 1:2000 in blocking buffer was added to the blot for 1 h. Prior to development, the blot was washed 4 times in wash buffer for 10 min and once in detection buffer (100 mM Tris-HCl, pH 9.5, 100 mM NaCl, and 5 mM $MgCl_2$) for 2 min. The blot was developed in detection buffer containing 0.45% NBT and 0.45% X-phosphate (Roche). Development was stopped by several changes of water.

Enzyme Assay Conditions and Analysis. (i) Zymography. Peptidoglycan was isolated from *P. aeruginosa* strain PAO1 as previously described (*32*, *33*). Purified peptidoglycan was incorporated into 12.5% polyacrylamide gels to a final concentration of 0.1%. Samples were subjected to electrophoresis, renatured in 0.1% Triton, and visualized as described elsewhere (*32*, *34*).

(ii) Turbidometry. The turbidometric assay of Hash (*35*) was used as previously described (*36*) to monitor the solubilization of either isolated and purified peptidoglycan from *P. aeruginosa* or whole cells of *Micrococcus luteus* (Sigma).

(iii) HPLC-Based Assay. The activity and product distribution catalyzed by LTs were followed by monitoring the release of soluble muropeptides from the insoluble substrate after enzyme treatment. Peptidoglycan isolated from *P. aeruginosa* as described above was further purified by treatment with α-amylase, DNase, RNase, and Pronase as described elsewhere (*37*). A typical enzyme assay reaction mixture contained 25 mM sodium acetate, pH 5.8, and 0.1% Triton in a total volume of 300 μL. Freeze-dried peptidoglycan was resuspended in the same reaction buffer, sonicated to prepare a homogeneous solution, and diluted to give a final substrate concentration of between 0.25 and 4.0 mg/mL. Reactions were initiated by the addition of enzyme followed by incubation at 37 °C with gentle shaking for 2 h. Undigested peptidoglycan was removed by ultracentrifugation at 100000*g* for 20 min at 24 °C [Beckman Airfuge, Beckman Instruments (Canada) Ltd., Mississauga, ON], and the soluble muropeptides recovered in the supernatants were resolved by high-pH anion-exchange chromatography (HPAEC) on a CarboPac PA1 column (4 × 250 mm; Dionex Canada Ltd., Oakville, ON) with pulsed amperometric detection. The column was equilibrated with 15 mM NaOH at 1 mL/min, and 20 min after sample injection, successive linear gradients to 100, 200, and 800 mM sodium acetate, each in 150 mM NaOH, were applied over 10, 20, and 20 min, respectively, to achieve resolution of muropeptides. The column was then washed in the final 800 mM sodium acetate, 150 mM NaOH for 15 min, and finally reequilibrated in the 15 mM NaOH. The pulsed-amperometric detector had electrode potentials set as follows: E_1, 0.13 V; E_2, 0.6 V; E_3, −0.6 V; with 500, 10, and 5 ms applied durations, respectively, and integration from 300 to 500 ms.

The assignment of molecular weight of three well-isolated soluble muropeptides form MltB(His_6)-digested peptidoglycan was made by ESI-MS. Samples eluted from HPAEC were passed through an on-line self-regenerating suppressor cartridge (Dionex) to remove the majority of buffer salts prior to further desalting by reverse-phase HPLC using a 4.6 × 150 mm Ultrashpere ODS column (Beckman). Samples were applied to the column, previously equilibrated in 0.1% trifluoroacetic acid, at a flow rate of 0.6 mL/min, and after buffer salts eluted in the void volume (5 min), the muropeptides were recovered with the application of 100% methanol. Detection was accomplished by UV absorbance at 210 nm.

Substrate Specificity of LTs. The ability of purified LTs to digest various peptidoglycan chemotypes and other polysaccharides of related structure was measured by a zymodot analysis (*38*). Briefly, this involved the incorporation of purified peptidoglycan of chemotypes A1γ (*E. coli*, *P. aeruginosa*, *Bacillus subtilis*), A2α (*M. luteus*), and A3γ (*Staphylococcus aureus*), cellulose, chitin, or casein (included as a control for peptidolytic activity) into 1% agarose and the application of enzyme-impregnated paper disks onto its surface. The enzymes tested were sMltB-His_6, SltB-His_6, hen egg-white lysozyme, and mutanolysin. After incubation, activity was judged after staining with methylene blue zymogram staining solution. Enzyme samples boiled for 1 h prior to assay served as negative controls.

The effect on LT activity of the presence of *O*-acetyl groups on peptidoglycan was tested by preparing the naturally *O*-acetylated material from *Proteus mirabilis* P19 as previously described (*33*, *39*). The extent of *O*-acetylation was determined by organic acid analysis HPLC after samples of purified peptidoglycan were subjected to mild-base hydrolysis (*33*, *39*). The specific activities of hen egg-white lysozyme, mutanolysin, and sMltB-His_6 toward the *O*-acetylated peptidoglycan and material that had been chemically de-*O*-acetylated by mild-base hydrolysis were determined using the kinetic assay described below (Kinetic Analysis of LTs).

The ability of LTs to digest chitooligosaccharides (degree of polymerization 2−6; Toronto Research Chemicals, Toronto, ON) and their 4-methylumbelliferyl derivatives (chitobiose, chitotriose) was investigated by their incubation (1 mM, final concentration) with sMltB-His_6 in 25 mM sodium acetate, pH 5.8, for 2 h at room temperature. The reaction products were analyzed by HPAEC as described above (HPLC-based assay).

Kinetic Analysis of LTs. A recently developed assay was employed for the kinetic analysis of the sMltB-His_6 and SltB-His_6 (*40*). Briefly, reactions were initiated as described above (HPLC assay), and at 5 min time intervals, aliquots were removed from the reaction mixture and quenched by plunging the sample into a dry ice/ethanol bath. At the appropriate time, the samples were thawed, and undigested peptidoglycan was immediately removed by ultracentrifugation (100000*g*, 15 min, 24 °C). Solubilized muropeptides in the supernatant were hydrolyzed to their constituent sugars by incubation in

6 M HCl for 1 h at 95 °C. The hydrolyzed samples were dried in vacuo and resuspended in sodium diluent (Beckman) for muramic acid detection. Muramic acid content was determined using a Beckman System Gold amino acid analyzer with ninhydrin detection as previously described (*39*). Initial activities were determined from plots of muramic acid content as a function of time, and expressed as nanomoles of peptidoglycan monomeric units (viz., GlcNAc-AnhMurNAc-peptide) released per minute. The Michaelis−Menten parameters were determined from plots of initial activity as a function of substrate concentration by nonlinear regression analysis using Enzfitter software (Biosoft, Cambridge, U.K.).

Other Analytical Techniques. Amino-terminal protein sequencing was performed on a Perkin-Elmer ABI 476A automated sequencer at the NAPS Unit, University of British Columbia, Canada. Protein concentration was determined using a bicinchoninic acid assay (Pierce, Rockford, IL). ESI-MS analysis of soluble muropeptides released from sMltB-His_6-digestion was performed using a quadropole MS in the ES+ mode at the Department of Chemistry, University of Waterloo, Canada.

RESULTS

Cloning and Mutation of Lytic Transglycosylases from P. aeruginosa. The nucleotide sequences of the *P. aeruginosoa* LTs were obtained by sequence alignments from the *Pseudomonas* genome project using *E. coli mltB*. These alignments revealed the existence of four separate ORFs encoding extensive amino acid identity with *E. coli* MltB. Of note is the presence of a single Cys followed by two Ser residues at positions 17 and 19 in one of the *P. aeruginosa* ORFs (Figure 3). This consensus sequence for protein lipidation in *E. coli* and related bacteria (*9, 41*) is absent in the other three identified ORFs. All hypothetical enzymes contain the putative catalytic glutamyl residue equivalent to Glu162 in the *E. coli* enzyme (Figure 3).

Based on the sequences obtained, appropriate oligonucleotide primers were synthesized for PCR amplification of the *P. aeruginosa mltB* gene and one of the three hypothetical genes encoding a nonlipidated form of MltB. Amplified genes were cloned into pET30a(+), and constructs pNBAC299-12 (full-length *mltB*) and pNBAC258-1 (full-length *sltB1*) were transformed into *E. coli* DH5α. The nucleotide sequences of both constructs including the plasmid-encoded hexa-histidine tag at the C-terminus of both translated proteins were confirmed prior to protein expression experiments.

Mutation of the chromosomal copies of *mltB* and *sltB1* in *P. aeruginosa* PAO1 was achieved by the insertion of a gentamicin resistance cassette within the ORFs of these genes using the allelic exchange strategy described by Schwiezer and Hoang (*26*). The plasmid constructs containing the interrupted LT genes were introduced into the mobilizer strain SM10 of *E. coli* by electroporation, and then conjugally transferred back into *P. aeruginosa*. Neither of these two knockout strains showed any noticeable change in cell phenotype compared to wild-type cells. Thus, there was no discernible difference between wild-type and mutated cells with respect to cell shape under phase microscopy, doubling time in LB, or the MIC values against carbenicillin (an antipseudomonal β-lactam antibiotic) (data not shown).

Expression and Purification of sMltB-His_6 and SltB1-His_6. Initial experiments to express MltB-His_6 from *P. aeruginosa*, using plasmid pNBAC299-12 which encoded the full-length enzyme with a C-terminal His-tag, resulted in poor expression levels using several hosts and induction conditions. The low-level expression of full-length MltB-His_6 could be followed after induction by Western immunoblot analysis using anti-His tag antibody. In an attempt to increase the expression levels, a second construct was made (pNBAC54-5) which encoded a deletion of the first 17 amino acids of MltB-His_6. The first 17 amino acids were chosen for deletion because this included the putative lipidation site, Cys17. This second construct would thus be a soluble form of an otherwise membrane-bound lipoprotein. To avoid confusion, we will refer to this protein as sMltB-His_6 to indicate its soluble nature. Recombinant sMltB-His_6 was expressed in *E. coli* BL21-λDE3 (pLysS) cells to levels sufficient for subsequent purification (Figure 4A).

Sufficiently high expression of full-length SltB1-His_6 was possible using construct pNBAC258-1 (Figure 4A). During protein induction of SltB1-His_6 at 37 °C with 1 mM IPTG, rapid cell lysis became apparent as judged by a decrease in viable plate counts. The induction temperature was subsequently decreased to 18 °C and the final concentration of IPTG was adjusted to 0.1 mM which allowed expression to continue without significant lysis.

The two soluble LTs (sMltB-His_6 and SltB1-His_6) were initially purified by immobilized metal affinity chromatography on Ni−NTA agarose. Lowering the pH of the buffer to 5.0 facilitated elution of sMltB-His_6 from the column, whereas SltB1-His_6 eluted at pH 5.5 (Figure 4A). Contaminating proteins, presumably nonspecifically adsorbed to the Ni−NTA agarose, were subsequently removed by cation-exchange chromatography. Both sMltB-His_6 and SltB1-His_6 with predicted p*I*s of 9.93 and 5.52, respectively, were separated using a Mono S FPLC column. The sMltB-His_6 protein eluted in approximately 1 M ammonium acetate, pH 8.0, while SltB1-His_6 eluted in 0.5 M of the same buffer. Finally, these buffers were exchanged for 10 mM ammonium acetate, pH 8.0, during a subsequent gel filtration chromatography on Superdex-75. A summary of the purification of both sMltB-His_6 and SltB1-His_6 is presented in Table 2.

During purification of SltB1-His_6, two bands of slightly differing molecular weight were consistently isolated and could not be separated with the protein purification procedure outlined above (Figure 4A). To determine the identity of these proteins, both were transferred to PVDF membranes, and the first 15 N-terminal amino acid residues were determined by sequencing. This revealed that the larger band corresponded to the full-length protein of SltB1-His_6, while the lower band matched SltB1-His_6 but starting at Gly30 (Figure 3). Analysis of SltB1 using SignalP V1.1 (http://genome.cbs.dtu.dk/services/SignalP/), which predicts signal sequence cleavage sites of proteins in *E. coli*, indicated that SltB1 should be cleaved between Ala29 and Gly30. Taken together, this would suggest that the doublet of bands copurified from SltB1-His_6-induced cells represents the enzyme with and without its attached N-terminal signal sequence. Since the full-length MltB-His_6 was not expressed to high enough levels, it is not clear if a similar processing took place in this enzyme, but no such doublet was visible in purified sMltB-His_6.

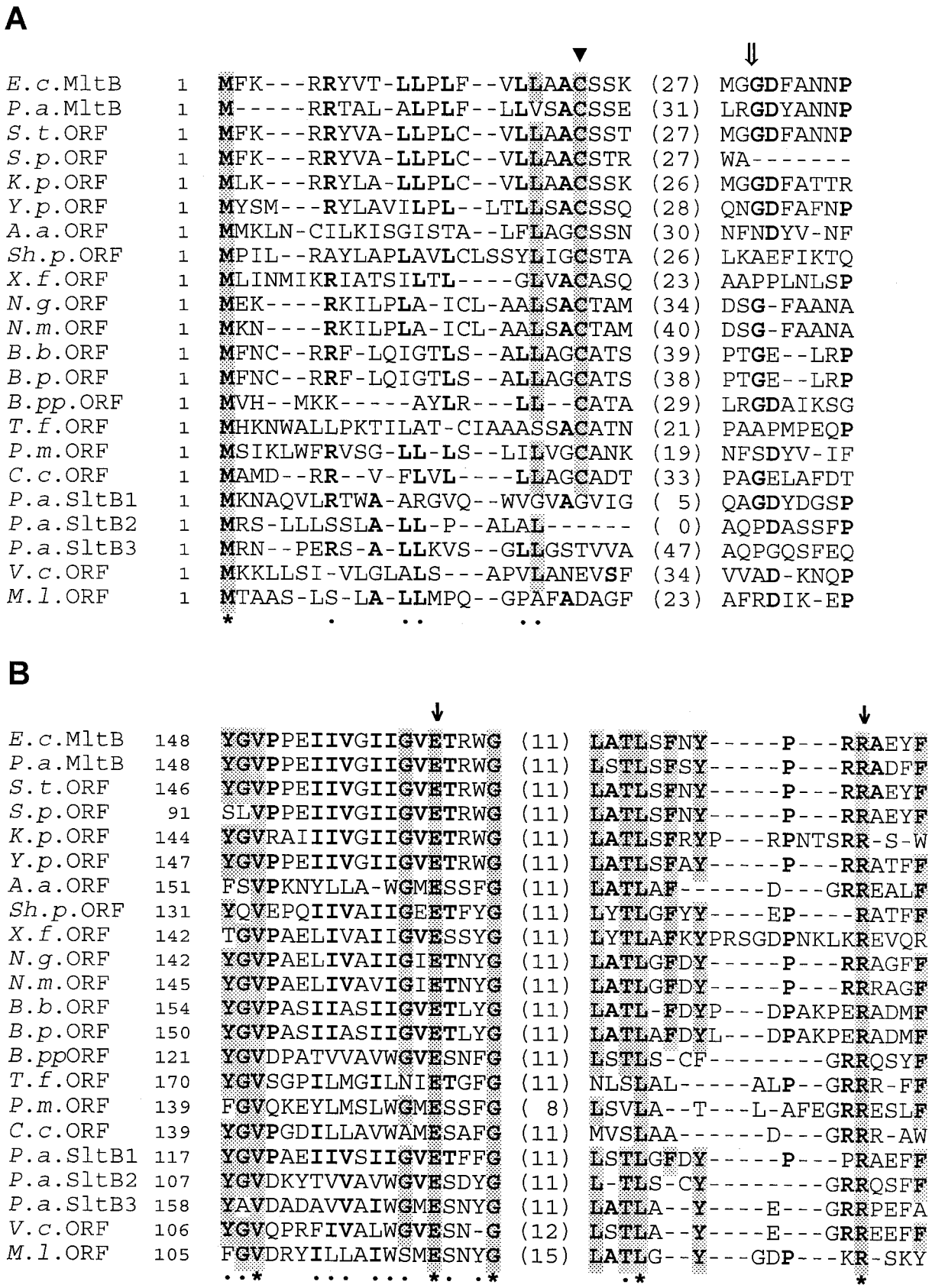

FIGURE 3: Amino acid sequence alignment of family 3 LTs. Residues shaded and boldface denote at least 80% and 50% identity, respectively, and the asterisks denote complete conservation. Panel A: the inverted triangle and the open arrow identify the putative lipidation and cleavage site, respectively. Panel B: the two arrows denote the putative catalytic Glu and substrate-binding Arg residues, respectively. Abbreviations: ORF, open reading frame; *E.c., E. coli*; *P.a., P. aeruginosa*; *S.t., Salmonella typhimurium*; *S.p., S. paratyphi*; *K.p., Klebsiella pneumoniae*; *Y.p., Yersinia pertussis*; *A.a., Actinobacillus actinomycetemcommitans*; *Sh.p., Shewanella putrefaciens*; *X.f., Xylella fastidiosa*; *N.g., Neisseria gonorrheae*; *N.m., N. meningitidis*; *B.b., Bordetella bronchiseptica*; *B.p., B. pertussis*; *B.pp., B. parapertussis*; *T.f., Thiobacillus ferroxidans*; *P.m., Pasteurella maltocida*; *C.c., Caulobacter crescentus*; *V.c., Vibrio cholerae*; *M.l., Mesorhizobium loti*.

Table 2: Purification of sMltB-His_6 and SltB-His_6 from *E. coli* BL21 (λDE3)[a]

enzyme	fraction	[protein] (mg·mL^{-1})	total protein (mg)	specific activity (nmol·min^{-1}·mg^{-1})	total activity (nmol·min^{-1})	purification(*x*-fold)	yield (%)
sMltB-His_6	cell lysate	5.30	53.0	44.1	2340	1	100
	Ni^{2+}−NTA agarose	1.02	6.12	90.5	554	2.05	23.6
	Mono S	0.083	0.330	535	177	12.1	7.54
SltB1-His_6	cell lysate	4.80	48.0	18.0	863	1	100
	Ni^{2+}−NTA agarose	1.40	8.42	35.6	299	1.97	34.6
	Mono S	0.045	0.180	1020	184	56.9	21.3

[a] The data presented are representative from 1 L of original cell culture.

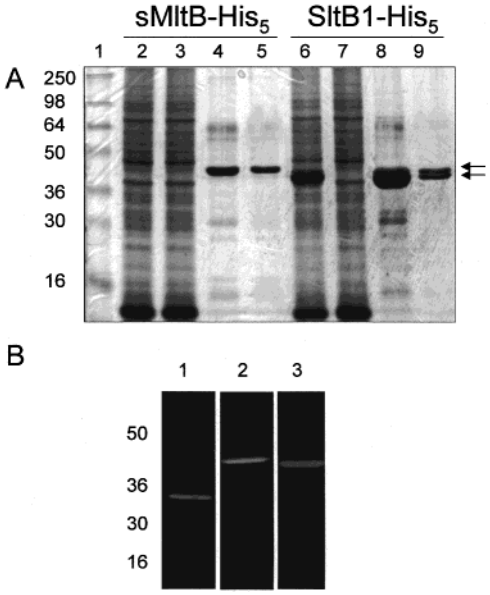

FIGURE 4: SDS−PAGE and zymogram analysis of sMltB-His_6 and SltB1-His_6. Panel A: SDS−PAGE analysis (Coomassie Brilliant Blue staining) of fractions obtained during purification of sMltB-His_6 and SltB1-His_6. Lanes: 1, molecular weight standards; 2,6, soluble cell lysates; 3,7, flow-through fractions from Ni^{2+}−NTA agarose; 4,8, elutions from Ni^{2+}−NTA agarose; 5,9, Mono S cation-exhange chromatographies. Arrows denote the two fractions of SltB1-His_6 that were blotted separately for N-terminal amino acid sequencing. Panel B: Zymogram analysis using purified *P. aeruginosa* peptidoglycan as substrate. After SDS−PAGE, the gel was incubated in 0.1% Triton to remove SDS and permit refolding of enzymes and subsequent in situ lytic activity of the peptidoglycan substrate. For visualization, the gel was stained with methylene blue, and zones of clearing denote lytic activity. Lanes: 1, 100 units of mutanolysin (positive control); 2, purified SltB-His_6; 3, purified sMltB1-His_6.

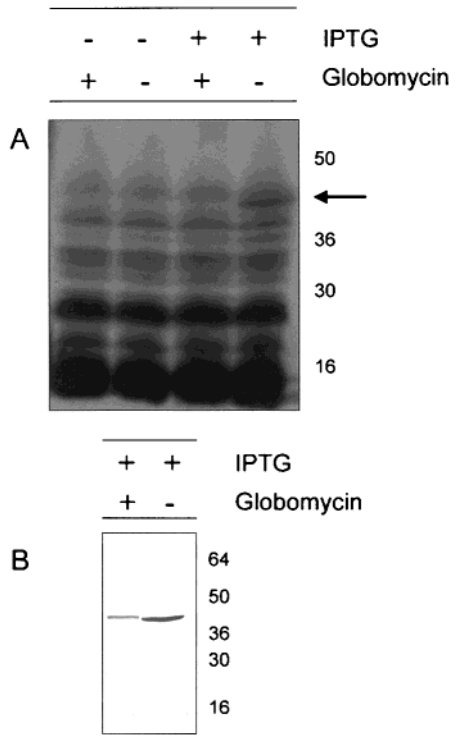

FIGURE 5: [^{3}H]Palmitate labeling and Western immunoblot analysis of *E. coli* proteins during expression of LTs. Panel A: autofluorograph of cell lysate samples during expression of full-length MltB-His_6 grown in the presence (+) or absence (−) of 0.1 mM IPTG and/or 100 μg/mL globomycin. The arrow denotes MltB-His_6. Panel B: Western immunoblot analysis of cell lysate samples during expression of full-length MltB-His_6 detected with an anti-His_5 primary antibody.

Lipoprotein Nature of Lytic Transglycosylases. Despite not being useful for protein purification studies because of poor expression, full-length MltB-His_6 was tested for labeling with [^{3}H]palmitate, which would indicate the recombinant protein is a lipoprotein. In addition, full-length SltB1-His_6 and sMltB-His_6 were also tested for lipoprotein labeling.

E. coli cell lysates containing the pET30a(+) expression plasmid contained several radioactive bands that were visible on autofluorographs after [^{3}H]palmitate labeling (Figure 5A). In addition to this lipoprotein profile, a protein with the expected molecular mass for MltB-His_6 of 40 kDa was detected by SDS−PAGE in lysates from MltB-His_6-expressing cells after induction with 0.1 mM IPTG. Furthermore, this labeling could be inhibited by the addition of 100 μg/mL globomycin, a signal peptidase-1 inhibitor. Incubation with globomycin did not, however, inhibit the expression of MltB-His_6, since protein could be detected in both induced cell preparations by Western immunoblot analysis using an anti-His tag antibody (Figure 5B). The Western immunoblot also revealed that globomycin-treated cells contained a His-tagged MltB protein with a slower migration compared with untreated cells. This observation indicated that a larger, prolipoprotein form of MltB-His_6 accumulated in these cells. As expected, deletion of the leader sequence of MltB-His_6, including the putative lipidated Cys17 in sMltB-His_6, completely abolished [^{3}H]palmitate labeling of the enzyme in the presence of IPTG (data not shown). A 39 kDa protein band was not observed in radiolabeled cells induced for SltB1-His_6, indicating that this is a naturally produced soluble LT.

Enzyme Activity. (i) Zymography. Renaturing SDS−PAGE analysis of purified sMltB-His_6 and SltB1-His_6 (Figure 4B) revealed that both enzymes retained their ability to degrade isolated, insoluble peptidoglycan from *P. aeruginosa* following the purification of protein from induced cells. Boiling sMltB-His_6 or SltB1-His_6 for 30 min prior to zymogram

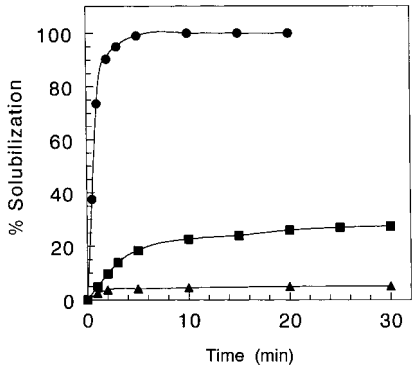

FIGURE 6: Turbidometric assay of peptidoglycan solubilization by sMltB-His$_6$ and lysozymes. Cells of *Micrococcus luteus* in 50 mM sodium phosphate buffer, pH 6.5, were incubated at 25 °C with (●) 2.5 units of HEWL, (■) 2.5 units of ostrich egg-white lysozyme, and (▲) sMltB-His$_6$. The decrease in A_{600} is expressed as a percentage of an appropriate control which lacked enzyme addition.

analysis abolished clearings within zymogram gels after renaturing. This indicated that the clearings in the zymograms were generated enzymatically and not due to a repulsion of the staining solution by the basic protein (*32*, *34*).

(ii) Turbidometry. The turbidometric assay of Hash (*35*) is based on monitoring the decrease in light scattering as insoluble peptidoglycan is cleaved into soluble products with the addition of lytic enzymes. Unlike the hydrolytic action of hen egg-white lysozyme, purified SltB1-His$_6$ was unable to catalyze the complete solubilization of either peptidoglycan from *P. aeruginosa* or a suspension of *Micrococcus luteus* cells (Figure 6). Instead, the enzyme caused an initial rapid but only partial decrease in turbidity. Interestingly, however, the progress curve of this activity resembled that generated by ostrich egg-white lysozyme, a member of the family 23 glycosidases (viz., goose-type lysozymes); again, complete solubilization was not achieved after an initial rapid burst of activity.

(iii) HPLC-Based Assay. A new protocol applying high-pH anion exchange chromatography (HPAEC) was developed to resolve mixtures of soluble muropeptides released from intact, insoluble peptidoglycan after treatment with sMltB-His$_6$ or SltB1-His$_6$. After enzyme treatment, insoluble substrate was removed by ultracentrifugation so that only solubilized muropeptides were analyzed. The HPAEC separation and resolution of muropeptides released after incubation with sMltB-His$_6$ for 30 min are shown in Figure 7A. As the supernatant of ultracentrifuged intact peptidoglycan was essentially free of muropeptides, the majority of peaks shown in Figure 7A arise from enzyme treatment. Three well-separated major peaks generated from sMltB-His$_6$ treatment were collected after HPAEC separation, desalted by reverse-phase HPLC, and analyzed by ESI-MS (Figure 7B). As expected, all three peaks contained disaccharides of GlcNAc and AnhMurNAc. The muropeptide that eluted from HPAEC at 64 min (peptide 3) was identified as cross-linked anhydrodisaccharide-tetrasaccharide [*m*/*z* calc 1829.9, *m*/*z* obs 1824.9 (Δ*m*, 5.0 Da)]. The other two peaks were characterized as disaccharides that varied in the length of their attached stem peptides [peptide 1, anhydrodisaccharide-pentapeptide: *m*/*z* calc 924.9, *m*/*z* obs 922.2 (Δ*m*, 2.7 Da); peptide 2, anhydrodisaccharide-tripeptide: *m*/*z* calc 853.9, *m*/*z* obs 851.3 (Δ*m* 2.6 Da)].

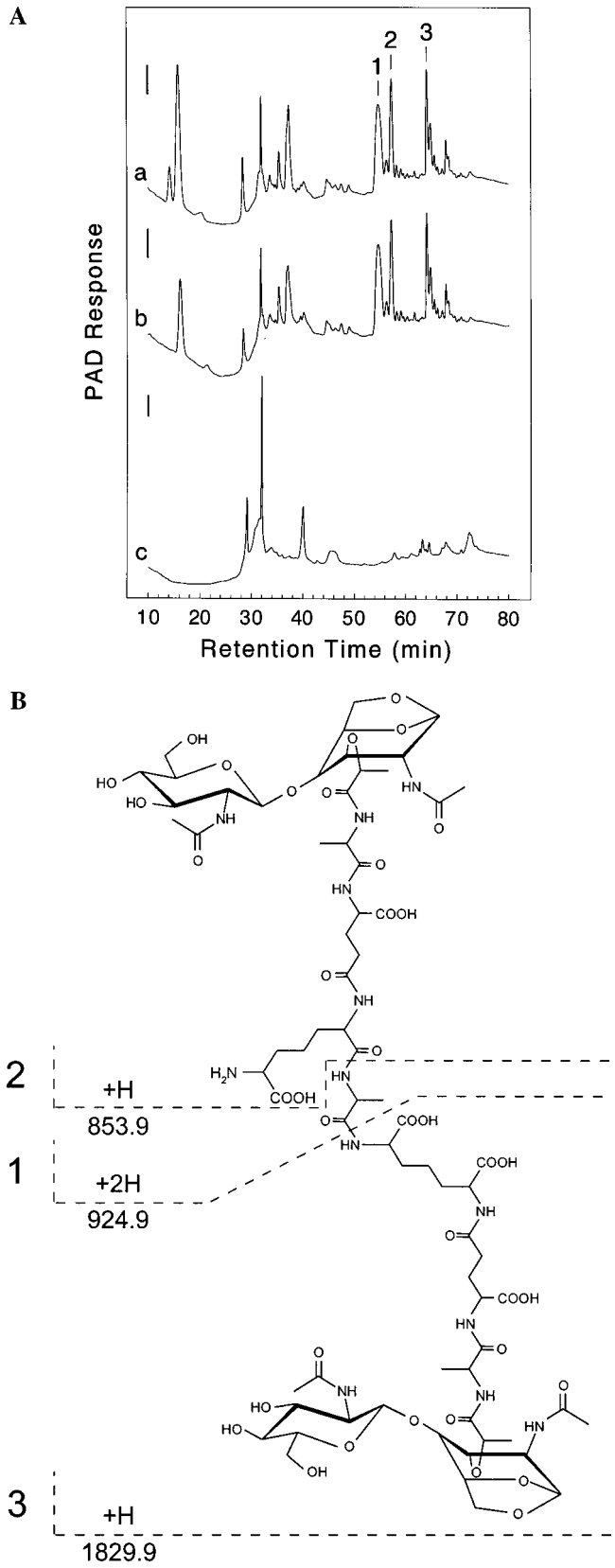

FIGURE 7: HPAEC separation of muropeptides released from peptidoglycan after treatment with LTs and the identification of major products by ESI-MS. Panel A: HPAEC chromatograms of muropeptides generated after treatment of peptidoglycan at pH 5.8 for 30 min with (a) sMltB-His$_6$, (b) SltB1-His$_6$, or (c) hen egg-white lysozyme. Peaks labeled 1−3 were collected, desalted by reverse-phase HPLC, and analyzed by ESI-MS. The solid bars denote 0.02 μCi. Panel B: Identification of three major products from chromatograms by ESI-MS.

Table 3: Effect of *O*-Acetylation on Susceptibility of Peptidoglycan to Cleavage by LT

	specific activity (nmol·min^{-1}·mg^{-1})[a]		
enzyme	de-*O*-acetylated	*O*-acetylated	% change
sMltB	373 ± 9.0	170 ± 11.5	−54.5
HEWL	291 ± 18.5	230 ± 11.2	−21.0
mutanolysin	108 ± 4.9	117 ± 3.6	+1.07

[a] ±SD (n = 3).

Table 4: Kinetic Properties of sMltB-His$_6$ and SltB1-His$_6$[a]

enzyme	K_M (μM)	k_{cat} (s^{-1})	k_{cat}/K_M (s^{-1}·M^{-1})
sMltB-His$_6$	72.1 ± 19.8	0.45 ± 0.122	6240
SltB1-His$_6$	181 ± 23.6	2.52 ± 0.372	13900

[a] Purified peptidoglycan from *P. aeruginosa* PA01 as substrate in 25 mM sodium acetate buffer, pH 5.8, containing 0.1% Triton at 37 °C; ±SD.

The HPAEC separation of SltB1-His$_6$-digested peptidoglycan resembled that of sMltB-His$_6$-digested material (Figure 7A). The three muropeptides identified by ESI-MS in sMltB-His$_6$ digests were also resolved in this profile. In contrast but as expected, digestion of *P. aeruginosa* peptidoglycan with hen egg-white lysozyme generated a very different soluble muropeptide profile (Figure 7A).

Substrate Specificity of Lytic Transglycosylases. Using a zymodot assay, both sMltB-His$_6$ and SltB-His$_6$ were found to be capable of degrading each of the samples of peptidoglycan with different chemotype (viz., A1γ, A2α, A3γ), but not cellulose, chitin, or casein (data not shown). As observed with zymography, boiling these enzymes prior to assay abolished all activity. Hen egg-white lysozyme and mutanolysin were also active toward chitin in addition to these different peptidoglycans.

As lytic transglycosylases form 1,6-anhydromuramyl residues as a product of their activity, a peptidoglycan partially substituted at the C-6 hydroxyl position of MurNAc with *O*-acetyl groups would be expected to be a poor substrate for these enzymes. To test this, peptidoglycan was isolated from *P. mirabilis* P19 and determined to be 52.8% *O*-acetylated, a value similar to that previously reported (*8*, *33*). This peptidoglycan and that chemically de-*O*-acetylated by mild-base hydrolysis were tested as substrates for sMltB-His$_6$, hen egg-white lysozyme, and mutanolysin. As seen in Table 3, the specific activities of both sMltB-His$_6$ and hen egg-white lysozyme were inhibited by the presence of *O*-acetyl groups on peptidoglycan, with the effect being greater on sMltB-His$_6$. Being a β-D−*N*,6-*O*-diacetylmuramidase, no such inhibition of activity was noted with mutanolysin.

Kinetic Analysis. The kinetics of both sMltB-His$_6$ and SltB1-His$_6$ activity against purified, insoluble *P. aeruginosa* peptidoglycan in 25 mM sodium acetate buffer, pH 5.8, containing 0.1% Triton were determined at 37 °C using a recently developed assay (*40*). This involved the recovery of soluble muropeptides from reaction mixtures over 30 min after addition of enzyme, and their subsequent quantification by amino acid analysis. Initial rates (velocities) of reaction were determined, and the Michaelis−Menten parameters established from these kinetic measurements are presented in Table 4. The apparent affinity of sMltB-His$_6$ for the peptidoglycan preparation was approximately 2.5 times greater than that of SltB1-His$_6$ for the same substrate, as reflected by values of K_M. However, the lower affinity of the latter enzyme for this substrate was compensated for by a greater turnover number compared to that for sMltB-His$_6$. These data indicated that of the two enzymes, SltB1-His$_6$ is more catalytically efficient as reflected by its k_{cat}/K_M value.

DISCUSSION

This is the first report of an autolysin from *P. aeruginosa* with specificity as a glycoside-cleaving enzyme. Previously, a D,D-carboxypeptidase (*42*) and a D,D-endopeptidase (*43*) specific for the pentaglycine cross bridges of *Staphlyococcus aureus* peptidoglycan have been characterized from *P. aeruginosa*. In addition, two extracellular autolysins that are expressed within naturally occurring membrane blebs during growth in vitro have also been described (*32*).

After cloning their genes, we expressed and purified two autolysins from *P. aeruginosa* PAO1 that share homology to the membrane lytic transglycosylase B protein of *E. coli*. MltB of *E. coli* is an outer membrane-localized lipoprotein that acts as an exo-enzyme cleaving the glycan strands of peptidoglycan in a progressive manner (*44*). It appears that in *E. coli*, MltB is proteolytically cleaved in vivo to produce a soluble, unlipidated form called Slt35 (*16*). Full-length *P. aeruginosa* MltB behaves like a lipoprotein as it displays globomycin-sensitive labeling with [^{3}H]palmitate. Removal of the first 19 amino acids from MltB, which included the presumed lipidation site of Cys19, created a soluble form of the enzyme which no longer labeled like the full-length isoform. However, it remains to be seen if the MltB of *P. aeruginosa* is cleaved in vivo during growth to yield a soluble form of this enzyme. SltB1 from *P. aeruginosa* also does not label with [^{3}H]palmitate and hence it is a naturally produced soluble family 3 enzyme.

Sequence alignments of the 22 family 3 LTs (Figure 3) reveal the presence of a Cys residue within the first 24 N-terminal residues of most of the hypothetical enzymes. In six of the cases, it is followed by Ser-Ser to provide the consensus lipidation sequence identified for *E. coli*. With a number of others, one or both Ser are replaced with Thr and/or Ala, but presumably these conservative changes still provide a lipidation site in the respective bacteria, suggesting that the enzymes would be MltBs. However, an N-terminal Cys residue is absent from the five remaining hypothetical LTs; three from *P. aeruginosa* and one each from *Vibrio cholerae* and *Mesorhizobium loti*. We have established here that one of these *P. aeruginosa* enzymes is indeed an SltB, and we are currently cloning the genes of the other two to provide protein for characterization. What significance, if any, these naturally produced soluble forms of MltB have in the biosynthesis and maintenance of peptidoglycan has yet to be established.

The genome of *P. aeruginosa* contains a total of four family 3 enzymes; MltB which is membrane-bound, and SltB1, SltB2 and SltB3 that are probably all soluble orthologues (*15*). It is not clear why this organism has the ability to produce so many family 3 enzymes, but redundancy in lytic transglycosylase genes is common in bacteria. Indeed, deletion of either *mltB* or *sltB1* from the *P. aeruginosa* chromosome did not lead to any phenotype, indicating that other still functional LTs may be able to compensate for the

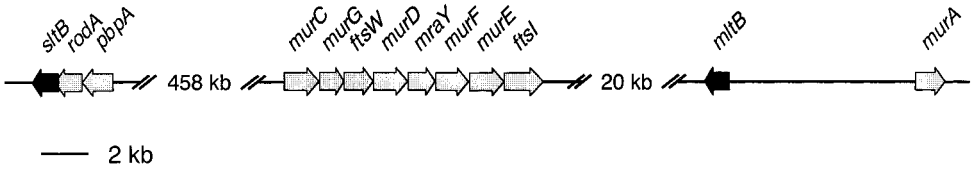

FIGURE 8: Physical map of the genetic loci involved in peptidoglycan biosynthesis. These loci span open reading frames PA4001 to PA4450 on the *P. aeruginosa* PAO1 chromosome. Only those open reading frames involved with peptidoglycan biosynthesis are depicted.

deletions. This result is supported by work in *E. coli* where mutants lacking up to eight autolysins apparently can still grow in vitro (*45*). It is believed that this redundancy reflects the importance of these gene products in cell physiology, analogous to the multiple penicillin-binding proteins that synthesize peptidoglycan. While this may be partly true, we also believe that bacteria contain a complement of lytic transglycosylase proteins to cleave the susceptible bond during different phases of growth or in different environments. This may be particularly important in organisms with ubiquitous lifestyles such as *P. aeruginosa* which can cause infection during both planktonic and biofilm modes of growth.

In this study we have shown that similar muropeptides are released from sMltB-His_6- and SltB1-His_6-digested peptidoglycan in vitro. Unfortunately, because it was not possible to produce enough full-length MltB-His_6 protein for subsequent investigations, it is unclear if the muropeptide profiles of a membrane-bound version of this enzyme would be different from those generated by its engineered soluble derivative, sMltB, or naturally occurring SltB1-His_6. Both of the LTs described here contain a domain with homology to the 'exo-loop' of Slt35 from *E. coli*. The 'exo-loop' is a 9 amino acid motif in Slt35 that projects into the active site cleft of the enzyme (*19*). It is thought that this domain might preclude endo-enzyme activity by this enzyme through steric hindrance with the stem peptides of the substrate. The similar profiles of muropeptide products produced by the two *P. aeruginosa* enzymes may be a reflection of this conserved domain. We are currently making site-directed replacements within the predicted 'exo-loop' domains of these enzymes to investigate if this affects the variety of muropeptide products produced.

All three major muropeptides released by sMltB-His_6 were anhydrosugar disaccharides as would be expected from an exo-acting LT. Reverse-phase HPLC has previously been used to resolve the soluble products of Slt35-treated peptidoglycan from *E. coli* (*16*). Using this technique, only two major muropeptides were observed: GlcNAc(β-1,4)-AnhMurNAc-tripeptide and GlcNAc(β-1,4)AnhMurNAc-tetrapeptide. However, development and application of an HPAEC-based analysis with pulsed amperometric detection led to the resolution of three major and at least seven minor muropeptides following sMltB-His_6 or SltB1-His_6 digestion of *P. aeruginosa* peptidoglycan. Interestingly, only one of the three major muropeptides was previously observed in the digests of *E. coli* MltB [viz., GlcNAc(β-1,4)AnhMurNAc-tripeptide]. It is not clear at present if these differences reflect differences in specificity between the *P. aeruginosa* and *E. coli* MltBs or subtle differences in the architecture of their respective peptidoglycan sacculi.

Using our recently developed kinetic assay involving a relatively convenient analysis for solubilized products (*38*), we have established the first Michaelis−Menten parameters for any LT. This fact is somewhat surprising given that this class of enzymes was first characterized over 25 years ago, and it means that we are unable to compare the catalytic activities of the *P. aeruginosa* enzymes with those from *E. coli.* While caution should be exercised when interpreting kinetic data obtained in vitro with homogeneous preparations of enzymes isolated from membranes and possibly multiprotein complexes, comparisons of their apparent properties can be made if they have been similarly treated. Some differences were observed in the kinetics of reactions performed by *P. aeruginosa* MltB and SltB which presumably reflect subtle differences in their structures. Studies on the specificity of action of LTs have revealed an absolute requirement for muramoyl residues and/or associated stem peptides on the substrate. For example, in contrast to muramidases, chitooligosaccharides do not serve as substrates for LTs (*40*), a finding confirmed in the current study using either chitin, chitooligosaccharides, or their 4-methylumbelliferyl derivatives. However, a crystal structure of bacteriophage lambda LT in complex with hexa-*N*-acetylchitobiose indicates that these ligands are capable of binding to the enzyme, but in a nonproductive manner (*46*). The four GlcNAc residues at the reducing end of the ligand were observed to occupy binding subsites A−D (−4 to −1). The reducing GlcNAc residue at subsite D (−1) was positioned slightly above the floor of the active site cleft and did not interact with Glu19, the acid catalyst positioned between subsites D (−1) and E (+1). Hence, it is likely that extra contacts involving the lactyl group of the muramyl residue in peptidoglycan substrates that would normally occupy this subsite and/or its associated stem peptide are required to position substrate at this site for catalytic cleavage. This view is supported by the three-dimensional structure of another complex, the *E. coli* Slt35 complexed with two molecules of GlcNAc-MurNAc-dipeptide (*22*). A number of contacts are apparent between the enzyme and the stem peptide of the ligand at subsite D (−1) including hydrogen bonding between Arg188 and the carbonyl of the lactyl moiety and a salt bridge between the free α-carboxyl group of the γ-glutamyl residue of the stem peptide and Arg187. Arg188 is totally conserved in the family 3 LTs (*15*), suggesting a key role in positioning substrate for subsequent cleavage. Like the *E. coli* enzyme, many of the family 3 LTs also possess an Arg at position 187 (Figure 3). This is the case for *P. aeruginosa* MltB1, but not for SltB where it is replaced with a proline. Thus, while many factors could contribute to substrate specificity and affinity, it is tempting to speculate that this second Arg at position 187 contributes to the greater apparent affinity of sMltB-His_6 compared to SltB1-His_6 as reflected by their respective K_M values. We are currently performing site-specific replacements of these and other

residues to further characterize the structure and function relationship of the *P. aeruginosa* LTs.

Unfortunately, little is known about the regulation of lytic transglycosylases, but we have made some interesting observations in the organization of family 3 LT genes in *P. aeruginosa*. Figure 8 depicts a segment of *P. aeruginosa* genome around *sltB1* and *sltB3*. *sltB1* is directly downstream from the genes encoding penicillin-binding protein 2 (*pbpB*) and RodA (*rodA*) which are known to interact in *E. coli* to control the rod shape of this organism (*47*). With the direct proximity of these genes to one another, it is tempting to speculate that they are coregulated and that their translation products form one of the multienzyme complexes thought to exist for peptidoglycan biosynthesis (*48*). However, this situation might be unique to *P. aeruginosa* because there is no equivalent organization of genes encoding PBPs and LTs in *E. coli* and preliminary studies with *E. coli* indicate that MltA and Slt70, but not MltB, complex with PBP2 and presumably RodA (*49*). In an effort to resolve this issue, we have initiated biochemical studies to investigate the nature of the associations, if any, involving the *P. aeruginosa* LTs and PBPs.

The organization of *mltB* within the *P. aeruginosa* genome is also intriguing (Figure 8). The *mltB* gene is located between the *mur* peptidoglycan synthetic operon, which has almost identical organization to that of *E. coli*, and the *murA* gene whose product initiates synthesis of the sacculus. The distances between these three elements may not seem significant until it is compared to those of *E. coli*. More than 2.7 megabases separate the *mur* operon and *mltB* on the chromosome of this latter is organism while *murA* is a further 0.5 megabase away from *mltB*.

The LTs appear to be enzymes with the substrate specificity of muramidases, a mechanism of action resembling the chitinases and related enzymes, but produce a unique reaction product which is capable of inducing a variety of pathobiological effects. The difference in their activity makes the LTs both interesting and, moreover, a suitable potential target for the development of a new class of antibacterials. An inhibitor with specificity for the LTs would target only bacterial and phage enzymes while not impacting a major factor of the innate immune system, viz. lysozyme.

ACKNOWLEDGMENT

We thank Kunitoshi Yamanaka and Masayori Inouye of the Department of Biochemistry, University of Medicine and Dentistry of New Jersey, Piscataway, NJ, for their generous gift of globomycin, and Sarah Sanowar for technical assistance.

REFERENCES

1. Höltje, J.-V. (1998) *Microbiol. Mol. Biol. Rev. 62*, 181−203.
2. van Heijenoort, J. (1998) *CMLS, Cell. Mol. Life Sci. 54*, 300−304.
3. Shockman, G. D., Daneo-Moore, L., Kariyama, R., and Massidda, O. (1996) *Microbial Drug Resist. 2*, 95−98.
4. Höltje, J.-V., and Tuomanen, E. I. (1991) *J. Gen. Microbiol. 137*, 441−454.
5. Höltje, J.-V. (1995) *Arch. Microbiol. 164*, 243−254.
6. Höltje, J.-V., Mirelman, D., Sharon, N., and Schwarz, U. (1975) *J. Bacteriol. 124*, 1067−1076.
7. Luker, K. E., Collier, J. L., Kolodziej, E. W., Marshall, G. R., and Goldman, W. E. (1993) *Proc. Natl. Acad. Sci. U.S.A. 90*, 12652−12658.
8. Clarke, A. J., and Dupont, C. (1992) *Can. J. Microbiol. 38*, 85−91.
9. Blake, C. C. F., Johnson, L. N., Mair, G. A., North, A. C. T., Phillips, D. C., and Sarma, V. R. (1967) *Proc. R. Soc. London, Ser. B 167*, 378−388.
10. Vocadlo, D. J., Davies, G. J., Lalne, R., and Withers, S. G. (2001) *Nature 412*, 835−838.
11. Mark, B. L., Vocadlo, D. J., Knapp, S., Triggs-Raine, B. L., Withers, S. G., and James, M. N. G. (2001) *J. Biol. Chem. 276*, 10330−10337.
12. Tews, I., Perrakis, A., Oppenheim, A., Dauter, Z., Wilson, K. S., and Vorgias, C. E. (1996) *Nat. Struct. Biol. 3*, 638−648.
13. Weaver, L. H., Grutter, M. G., and Matthews, B. W. (1995) *J. Mol. Biol. 245*, 54−68.
14. Knapp, S., Vocadlo, D., Gao, Z., Kirk, B., Lou, J., and Withers, S. G. (1996) *J. Am. Chem. Soc. 118*, 6804−6805.
15. Blackburn, N. T., and Clarke, A. J. (2001) *J. Mol. Evol. 52*, 78−84.
16. Engel, H., Smink, A. J., van Wijngaarden, L., and Keck, W. (1992) *J. Bacteriol. 174*, 6394−6403.
17. Ehlert, K., Höltje, J.-V., and Templin, M. F. (1995) *Mol. Microbiol. 16*, 761−768.
18. Dijkstra, A. J., Hermann, F., and Keck, W. (1995) *FEBS Lett. 366*, 115−118.
19. van Asselt, E. J., Dijkstra, A. J., Kalk, K. H., Takacs, B., Keck, W., and Dijkstra, B. W. (1999) *Structure 7*, 1167−1180.
20. Thunnissen, A. M. W. H., Dijkstra, A. J., Kalk, K. H., Rozenboom, H. J., Engel, H., Keck, W., and Dijkstra, B. W. (1994) *Nature 367*, 750−753.
21. van Asselt, E. J., Thunnissen, A. M. W. H., and Dijkstra, B. W. (1999) *J. Mol. Biol. 291*, 877−898.
22. van Asselt, E. J., Kalk, K. H., and Dijkstra, B. W. (2000) *Biochemistry 39*, 1924−1934.
23. van Asselt, E. J., and Dijkstra, B. W. (1999) *FEBS Lett. 458*, 429−435.
24. Govan, J. R. W., and Deretic, V. (1996) *Microbial Rev. 60*, 539−574.
25. Jollès, J., Périn, J.-P., and Jollès, P. (1977) *Mol. Cell. Biochem. 17*, 39−44.
26. Schweizer, H. P., and Hoang, T. T. (1993) *Gene 158*, 15−22.
27. Schweizer, H. P. (1993) *Bio/Techniques 15*, 831−833.
28. Hoang, T. T., Karkhoff-Schweizer, R. R., Kutchma A. J., and Schweizer, H. P. (1998) *Gene 212*, 77−86.
29. Simon, R., Priefer, U., and Pühler, A (1983) *Bio/Technology 1*, 784−791.
30. Ausubel, F. M., Brent, R., Kingston, R. E., Moore, D. D., Seidman, J. G., Smith, J. A., and Struhl, K. (1987) *Current Protocols in Molecular Biology*, John Wiley and Sons, New York.
31. Kraft, A. R., Templin, M. F., and Höltje, J-.V. (1998) *J. Bacteriol. 180*, 3441−3447.
32. Watt, S. R., and Clarke, A. J. (1994) *J. Bacteriol. 176*, 4784−4789.
33. Clarke, A. J. (1993) *J. Bacteriol. 175*, 4550−4553.
34. Bernadsky, G., Beveridge, T. J., and Clarke, A. J. (1994) *J. Bacteriol. 176*, 5225−5232.
35. Hash, J. H. (1967) *J. Bacteriol. 93*, 1201−1202.
36. Dupont, C., and Clarke, A. J. (1991) *Eur. J. Biochem. 195*, 763−769.
37. Glauner, B., and Schwartz, U. (1988) *Bacterial Cell Surface Techniques* (Hancock, I. C., and Poxton, I. R., Eds.) pp 158−168, John Wiley and Sons, New York.
38. Watt, S. R., and Clarke, A. J. (1997) *Can. J. Microbiol. 43*, 1054−1062.
39. Clarke, A. J. (1993) *Anal. Biochem. 212*, 344−350.
40. Blackburn, N. T., and Clarke, A. J. (2000) *Anal. Biochem. 284*, 388−393.

41. Braun, V., and Wu, H. C. (1994) in *Bacterial Cell Wall* (Ghuysen, J.-M., and Hakenbeck, R., Eds.) pp 319−341, Elsevier Science, New York.
42. Presslitz, J. E., and Ray, V. A. (1975) *Antimicrob. Agents Chemother. 7*, 578−581.
43. Brito, N., Falcon, M. A., Carnicero, A., Gutierrez-Navarro, A. M., and Mansito, T. B. (1989) *Res. Microbiol. 140*, 125−137.
44. Romeis, T., Vollmer, W., and Höltje, J-.V. (1993) *FEMS Microbiol. Lett. 111*, 141−146.
45. Höltje, J-.V., and Heidrich, C. (2001) *Biochimie 83*, 103−108.
46. Leung, A. K.-W., Duewel, H. S., Honek, J. F., and Berghuis, A. M. (2001) *Biochemistry 40*, 5665−5673.
47. Matsuhashi, M. (1994) in *Bacterial Cell Wall* (Ghuysen, J.-M., and Hakenbeck, R, Eds.) pp 55−71, Elsevier, New York.
48. Höltje, J.-V. (1998) *Microbiol. Mol. Biol. Rev. 62*, 181−203.
49. von Rechenberg, M., Ursinus, A., and Höltje, J.-V. (1996) *Microbial Drug Resist. 2*, 155−157.
50. Hancock, R. E. W., and Carey, A. M. (1979) *J. Bacteriol. 140*, 902−910.

BI011833K